SwarmNet:
A Distributed Navigation Network using Ultra Wideband Ranging and Communications

Brandon Dewberry
Time Domain
Huntsville, Alabama, USA
info@timedomain.com

Alan Petroff
Time Domain
Huntsville, Alabama, USA
info@timedomain.com

***Abstract*—Ultra Wideband (UWB) radios use a pulsed-RF signaling structure to provide multipath-resistant peer-to-peer distance measurement between radio transceivers. Recent breakthroughs have introduced small, low power, and highly accurate ranging radios to the market. This paper reports a mathematical and algorithmic foundation for networking these transceivers such that the driving force behind the network optimization is no longer data throughput or routing, but instead localization accuracy. This tightly-coupled navigation scheduler and communication protocol has been dubbed "SwarmNet".**

The SwarmNet framework combines error-driven scheduling with navigation accuracy optimization through distributed Extended Kalman Filters (EKF) with novel sharing of location and error covariance across neighboring nodes. Experimental testbed results show slotted ALOHA capacity can be sufficient when other navigation sensors are utilized. Simulation of multiple cooperative nodes demonstrate "accuracy flooding" where transient dimensional accuracy is propagated through independent mobile agents.

Keywords—Ultra Wideband (UWB); ALOHA network; Extended Kalman Filter (EKF); Mobile Ad-hoc Tracking Networks (MATNET)

I. INTRODUCTION

UWB radio uses a pulsed-RF signaling structure rather than sinusoids to provide multipath-resistant peer-to-peer distance measurement between radio transceivers. The recent availability of small, low power, affordable pulsed-RF UWB transceivers [1,2] provides the basis for renewed interest in distributed localization for multi-agent cooperative field robotics.

While it seems intuitive that accurate peer-to-peer distance measurements in high multipath environments could revolutionize cooperative field robotics in GNSS-compromised environments, a network protocol is required that emphasizes localization accuracy over data throughput. In addition each precision range measurement is a unicast (as opposed to broadcast) time-of-flight packet conversation and each requires a finite amount of time, so measuring the complete network link space is prohibitive in a dynamic system. Finesse is required in the network to make sure agents optimize their own ranging opportunities and minimize interference with distant agents. This mobile ad-hoc navigation network protocol, dubbed "SwarmNet" is the subject of this report.

SwarmNet uses a combination of pulsed-RF peer-to-peer ranging, communications, and Kalman navigation. It addresses the difficult problem of dynamic localization in mobile ad-hoc systems through dynamic cooperation among network agents. Any field robotics application typically based on GNSS navigation could be safer and more autonomous through added peer-to-peer measurements provided by SwarmNet. A few of these applications are illustrated in fig. 1.

II. BACKGROUND

A. Signal Model

The SwarmNet protocol is based on a pulsed-RF

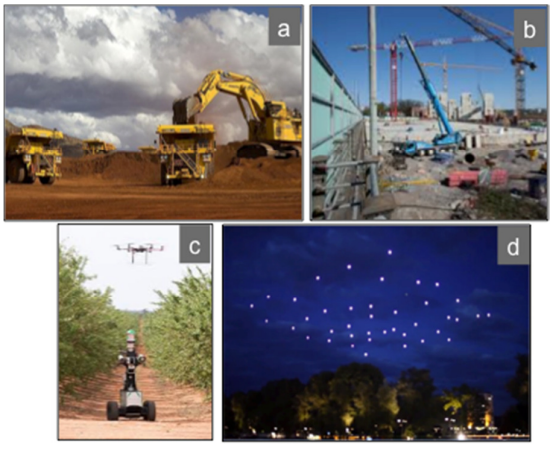

Ultra Wideband signal with time and frequency representation as depicted in figure 2. This signaling strategy is optimized toward accurate measurement of the time of arrival (TOA) of the signal at the receiver while also respecting FCC and EU regulatory limits. This signaling basis can be modeled as a N-cycle

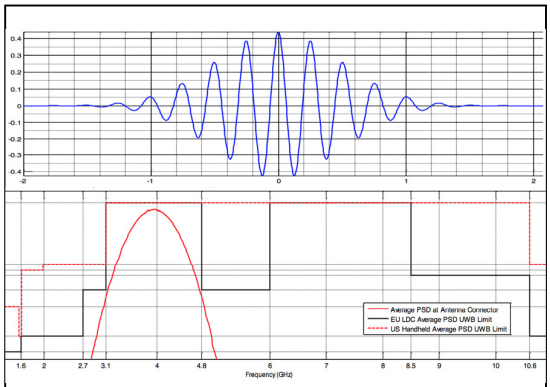

Fig. 2. The time and frequency representation of the basis signal. The signal shape is optimized toward brevity in time while sinusoid with Gaussian envelope allowing separate control of center frequency and bandwidth [3].

This signaling basis is structured into packets consisting of a stream of pulses separated by pseudo-random delays in order to support channelization as well as low duty cycle limits. Specifically this time-hopping structure can modeled as follows (derived from [4]):

$$s_{tr}^{(k)} = A_k \sum_{j=-\infty}^{\infty} d_{\lfloor \frac{j}{N_s} \rfloor}^{(k)} w_{tr}\left(t^{(k)} - jT_f - c_j T_c\right),$$

where:

A_k is an amplitude normalization factor,

w_{tr} is the transmitted basis waveform,

$t^{(k)}$ is the k[th] transmitter's clock time,

T_f is the mean pulse repetition interval (PRI),

$\{c_j\}$ is a time hopping sequence, common to transmitter and receivers on the same channel,

T_c is the duration of delay based on the repeating pattern at index c, and

$\{d_{\lfloor \frac{j}{N_s} \rfloor}^{(k)}\}$ is a binary modulation sequence from the binary set [-1,1] implementing bi-phase shift keying or "flip" modulation with symbol dwell duration N_s.

N_s pulses are transmitted for each symbol, this series energy summed together at the receiver in a coherent integration process. Coherent pulse integration is often used in radar and GNSS receivers in order to increase Signal to Noise Ratio (SNR) through process gain at the expense of measurement rate. [5]. Separate sequences (code and pulse integration) are used for acquisition, demodulation, and waveform scanning allowing each of these packet frames to support meet separate SNR and coding requirements.

B. Two Way Time of Flight (TW TOF) Ranging

A transmitted packet is acquired and demodulated by nearby receivers that lock, demodulate, and scan the pulse waveform in order to measure the Time of Arrival (TOA) of the first, most direct pulse. This compression of an entire packet into a direct-path timing event is central to accurate distance measurement. A Two-Way Time-of-Flight (TW TOF) protocol, as depicted in figure 3, implements this compression process twice, first during request packet reception and again during response packet reception. The result is a phase delay measurement in the initiating (requesting) radio which computes a distance estimate based on this conversation delay minus the computation time (τ_{delay}) which is pre-configured and known in both the requester and responder [1,2,7]:

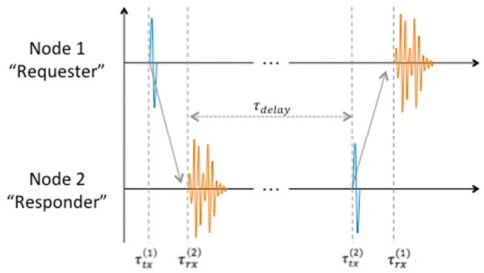

Fig 3. Timeline of the Two-Way Time-of-Flight (TW TOF)

$$\hat{r}_{1,2} = \frac{c}{2}\left(\tau_{rx}^{(1)} - \tau_{tx}^{(1)} - \tau_{delay}\right)$$

III. SWARMNET ARCHITECUTURE

The embedded architecture implemented in each SwarmNet node is depicted in figure 4. Based on a foundation of TW TOF ranging and communication, each node implements:

a. Scheduler
b. Neighbor Database (NDB)
c. *Range Target Prioritization (RTP)*
d. EKF Localization

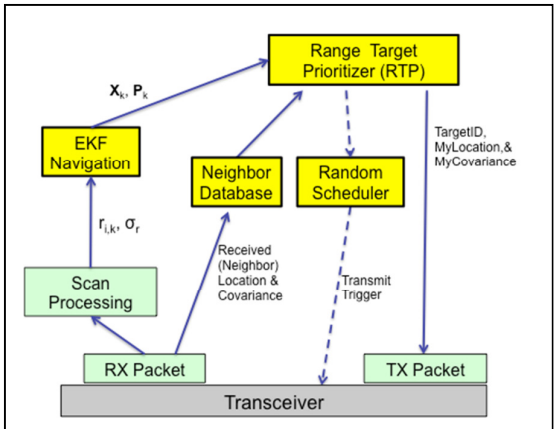

Fig 4. The SwarmNet embedded architecture. The components in yellow (and bold outline) comprise the SwarmNet enhancement.

A. *Scheduler*

Pulsed signaling with distance measurement has the potential to provide extended network data capacity and robustness [6,7]. However these analyses are focused primarily on data throughput and routing. A navigation network will maximize the location accuracy of all network nodes.

In Mobile Adhoc Networks central coordination is problematic. Thus for fully mobile navigation networks with low capacity requirements a scheduling scheme based on slotted random-access (ALOHA) scheduling can be considered.

Slotted ALOHA provides a theoretical network capacity of 36% [8]. While enhanced methods are possible navigation networks in field applications have the possibility of decreasing the required capacity through aiding sources such as inertial navigation or odometry. Also Range Target Prioritization (RTP) complements the scheduler by maximizing the information provided in each range conversation.

B. *Neighbor Database (NDB)*

The Neighbor Database is simply a list, maintained in each node, of all nodes heard in the last T_{ndb} seconds. An active process maintains the age of the latest transmission from each node and culls the list as necessary.

This object database also includes the latest estimate of location and location error (covariance) of the associated node (if available) as published by each node in support of the SwarmNet protocol.

C. *Range Target Prioritization (RTP)*

When the scheduler triggers a transmission the RTP selects the target responder from the NDB list. This selection is based on an accuracy optimization strategy.

Fig. 5 illustrates this optimization process. In this simplified example the node at the origin is under test and has eight neighboring nodes from which to choose, all with various relative directions and covariance represented by 2D error ellipses. These relative range and bearings along with covariance estimates are computed from data provided by the neighbors and stored in the Neighbor Database.

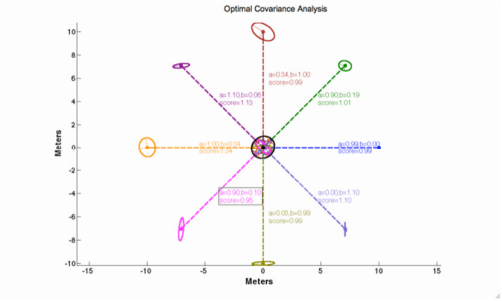

Fig. 5. The RTP algorithm in the center node selects which node minimizes its error ellipse based on the relative direction and covariance of neighbors.

The SwarmNet airtime protocol has each node publish its own location and error estimates in range response packets. A weighted optimization strategy such as Kalman estimation is used to estimate the covariance that would result from ranging to each neighbor. The minimum trace of the error ellipses formed from a posteriori covariances provides the minimum error prediction.

D. *Distributed Kalman Navigation*

Optimal recursive Kalman estimation is a well-established technique for navigation [11]. Because Euclidean distance is a nonlinear operation this technique uses a discrete time Extended Kalman Filter with linearized H matrix. For a 2D implementation these components are:

$$\mathbf{X}_k = \begin{bmatrix} \bar{x}_k \\ \dot{x}_k \\ y_k \\ \dot{y}_k \end{bmatrix}, \quad \mathbf{P}_k = \begin{bmatrix} \boldsymbol{var(x_k)} & cov(x_k, \dot{x}_k) & \boldsymbol{cov(x_k, y_k)} & cov(x_k, \dot{y}_k) \\ cov(x_k, \dot{x}_k) & var(\dot{x}_k) & cov(\dot{x}_k, y_k) & cov(\dot{x}_k, \dot{y}_k) \\ cov(x_k, y_k) & cov(\dot{x}_k, y_k) & \boldsymbol{var(y_k)} & cov(y_k, \dot{y}_k) \\ cov(x_k, \dot{y}_k) & cov(\dot{x}_k, \dot{y}_k) & cov(y_k, \dot{y}_k) & var(\dot{y}_k) \end{bmatrix},$$

$$\mathbf{H}_k = \begin{bmatrix} \frac{x_k - x_0}{\bar{r}} & 0 & \frac{y_k - y_0}{\bar{r}} & 0 \end{bmatrix}$$

where (x_k, y_k) is the a priori 2D location estimate at time instance k and (x_0,y_0) is the reference location. Each agent participates in the SwarmNet protocol by broadcasting the five highlighted data components x_k, y_k, $var(x_k)$, $var(y_k)$, & $cov(x_k, y_k)$ in each range response packet, providing neighbors with potential reference locations and location error estimates.

IV. METHODS

A mobile adhoc navigation network simulation environment was developed. In addition a network testbed consisting of nine PulsON P400 UWB transceivers from Time Domain was developed.

V. RESULTS

A. *UWB Random Scheduling*

Fig. 6 illustrates the capacity found in our UWB slotted random ranging scheduler test bed. As the number of nodes increased, the drop off in throughput was consistent with a capacity of 36%. This validates the theoretical limit of slotted ALOHA.

Typical random-access "ALOHA" experiments analyze many transmitters and one receiver [7]. However full ranging conversations require a request followed by response packet. After an initial set of experiments we found the turnaround time between request and response packet to be critical. If a rogue transmitter happens to send a request during this critical time just after request, the requesting radio will acquire the wrong packet and the conversation measurement fails.

Thus the network algorithm was enhanced with a Virtual Carrier Sense (VCS) mechanism common to narrowband networks in order to improve the hidden node phenomenon [12].

B. *Simulation Results*

Fig. 7 provides a detailed visual comparison of simulation results with mobiles ranging strictly to references R1 and R2 (a) versus enabling ranging to other mobiles (b). The "true" (simulated) location of M3 is dotted orange. The Kalman location estimate and covariance are represented by grey dots and 2D ellipses, respectively. As the two experiments indicate, the addition of mobile-to-mobile ranging greatly improves the systemic and statistical errors as well as the covariance estimation of each network agent.

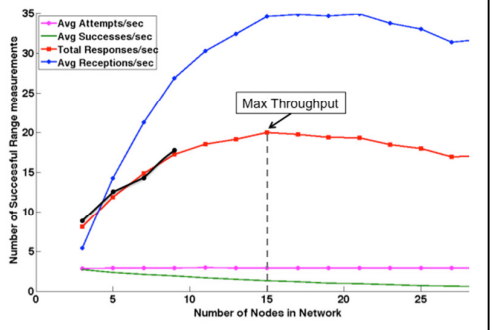

Fig 6. A network 3Hz mean ranging rate and 20ms airtime duration per range measurement produces maximum throughput with 15 nodes. This relates to roughly 40% capacity using purely random scheduling

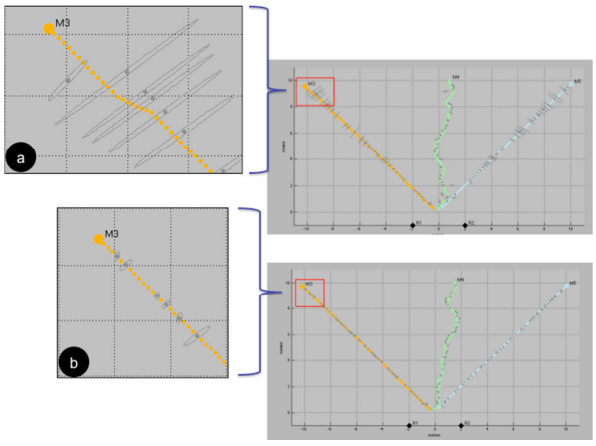

Fig. 7. Simulation results (a) without peer-to-peer mobile referencing and (b) with peer-to-peer mobile referencing. In (b) the Kalman state and covariance is improved by optimal ranging to neighboring cooperative mobile agents with better geometry.

VI. DISCUSSION

The SwarmNet protocol is quite flexible. In particular it supports ad-hoc deployment of references and fully mobile field agents. Each agent chooses dynamically and in real time which neighboring node to use as reference. Nodes with good accuracy will advertise this through a lower error in their published covariance. Neighboring nodes will naturally utilize these references. Thus safety and precision maneuvering areas can be set up "on the fly" or provided by special support vehicles. Accuracy floods through the network until propagation errors limit its usefulness.

VII. CONCLUSION

The "SwarmNet" protocol, a tight coupling of UWB ranging with Kalman navigation and a location accuracy-driven network provides a ideal framework for enabling a novel navigation network.

REFERENCES

[1] Johnson, J., & Dewberry, B., "UltraWideband Aiding of GPS for Quick Deployment of Anchors in a GPS-denied Ad hoc Sensor Tracking and Communications System", Proceedings of the 2001 Institute of Navigation Global Navigation Satellite Systems, ION GNSS, 19-23 September, 2011, Portland, OR

[2] Dewberry, B., & Beeler, B., "Realtime Range Error Estimation from Pulse Waveform Signature Analysis in Support of Extended Kalman Filter-based Indoor Navigation", Proceedings of the Institute of Navigation (ION) 2011 Joint Navigation Conference, 26-28 June, 2011, Colorado Springs, CO

[3] Miller, L.E., "Models for UWB pulses and their effects on narrowband direct conversion receivers", Proceedings of the IEEE International Conference on Ultra Wideband Systems and Technologies, 2003

[4] Scholtz, R.A., Pozar, D.M. and Namgoong W., "Ultra-Wideband Radio," EURASIP Journal on Applied Signal Processing, 2005:3, pp. 252-272

[5] Richards, M.A., "Coherent integration loss due to white Gaussian phase noise," *Signal Processing Letters, IEEE* , vol.10, no.7, pp.208,210, July 2003

[6] Venkatesh, S.; Buehrer, R.M., "Multiple-access design for ad hoc UWB position-location networks," *Wireless Communications and Networking Conference, 2006. WCNC 2006. IEEE* , vol.4, no., pp.1866,1873, 3-6 April 2006

[7] Kheiri, F., Dewberry, B., Joiner, L., and Wu, D., "Capacity Analysis of an Ultrawideband Active RFID System," Proc. IEEE SoutheastCon 2008, April 2008, Huntsville, AL.

[8] Namislo, C., "Analysis of Mobile Radio Slotted ALOHA Networks," *Selected Areas in Communications, IEEE Journal on* , vol.2, no.4, pp.583,588, July 1984

[9] W. M. Lovelace, J. K. Townsend, "Threshold Discrimination and Blanking for Large Near Far Power Ratios in UWB Networks," IEEE Transactions on Communications, in press, April, 2005.

[10] Roberts, L. G. "ALOHA Packet System With and Without Slots and Capture". Computer Communications Review 5 (2): 28–42. April 1975.

[11] Simon, Dan (2006). Optimal State Estimation. Hoboken, NJ: John Wiley & Sons.

[12] Fu-Yi Hung; Marsic, I., "Effectiveness of Physical and Virtual Carrier Sensing in IEEE 802.11 Wireless Ad Hoc Networks," *Wireless Communications and Networking Conference, 2007.WCNC 2007. IEEE* , vol., no., pp.143,147, 11-15 March 2007